Available online at www.sciencedirect.com
SCIENCE DIRECT®
J. Chem. Thermodynamics 35 (2003) 955–965
JCT
www.elsevier.com/locate/jct

Low temperature heat capacity of $Nd_2Zr_2O_7$ pyrochlore

S. Lutique [a], P. Javorský [a], R.J.M. Konings [a,*], A.C.G. van Genderen [b], J.C. van Miltenburg [b], F. Wastin [a]

[a] *European Commission, Joint Research Centre, Institute for Transuranium Elements, P.O. Box 2340, 76125 Karlsruhe, Germany*
[b] *Chemical Thermodynamics Group, Utrecht University, Padualaan 8, 3584 CH, Utrecht, Netherlands*

Received 28 October 2002; accepted 4 February 2003

Abstract

Heat capacity of neodymium zirconate ($Nd_2Zr_2O_7$) with pyrochlore structure was measured by adiabatic calorimetry and the hybrid adiabatic relaxation method in the temperature range (0.45 to 400) K. Its excess component was obtained by comparison with the heat capacity of the lanthanum zirconate. A thermal anomaly was observed below $T = 7.2$ K. From the heat capacity measurements, the thermodynamic functions of $Nd_2Zr_2O_7$ were determined.

Keywords: Pyrochlore; Neodymium zirconate; Heat capacity; Thermodynamic properties

1. Introduction

Pyrochlores with the general formula $A_2B_2O_7$ have many potential technological applications because of their refractory nature and their interesting electronic properties, which vary from insulating through semiconductor to metal-like depending on the chemical composition [1]. Lanthanide pyrochlores, in which the light lanthanide elements (La to Gd) can occupy the A position, are well known for their magnetic behaviour at low temperature and their fluorescent phosphorescent behaviour [1].

* Corresponding author. Tel.: +49-7247-951-391; fax: +49-7247-951-566.
E-mail address: konings@itu.fzk.de (R.J.M. Konings).

0021-9614/03/$ - see front matter
doi:10.1016/S0021-9614(03)00040-5

In nuclear technology there has been a lot of attention paid to zirconate and titanate pyrochlores (B = Ti or Zr) and related compounds like zirconolite because of their capability to incorporate not only lanthanides but also actinides. Such compounds have been proposed for plutonium or the minor actinides [2,3] as their natural analogues have shown to be very durable over very long time periods. The thermodynamic stability is a key parameter for modeling the durability and knowledge of the fundamental thermodynamic properties is thus essential.

Only a few studies of the thermodynamic properties of the lanthanide zirconate pyrochlores have been reported. Korneev *et al.* [4] measured the molar enthalpies of formation of the series of $La_2Zr_2O_7$, $Pr_2Zr_2O_7$, $Nd_2Zr_2O_7$, and $Sm_2Zr_2O_7$, Bolech *et al.* [5–7] the molar enthalpy of formation of $La_2Zr_2O_7$, and Helean *et al.* [8] of $Gd_2Zr_2O_7$. The heat capacity of $La_2Zr_2O_7$ and $Ce_2Zr_2O_7$ {in the temperature range (5 to 900) K} was studied by Bolech *et al.* [5,7] and in a recent paper we have reported the high-temperature heat capacity ($T = 300$ K to $T = 1600$ K) of $Nd_2Zr_2O_7$ [9]. The present paper extends our work with low temperature measurements in the temperature range (0.45 to 400) K.

2. Experimental

Neodymium zirconate was obtained by co-precipitation from a solution of zirconium oxi-chloride $ZrOCl_2 \cdot 8H_2O$ and neodymium nitrate $Nd(NO_3)_3 \cdot 6H_2O$ (Alfa Aesar) of stoichiometric concentration which was adjusted to pH 11 by addition of ammonia. The powder thus obtained was sintered for 72 h at $T = 1923$ K in air. Pellets were obtained by pressing calcined beads prepared by the sol–gel method, followed by sintering, as described in detail previously [9]. The pellet density was 97% of the theoretical density ($6325\,kg \cdot m^{-3}$). X-ray analysis proved the products to be pure, revealing a cubic pyrochlore phase (Fd3m space group) with lattice parameter a of 1.07 nm.

Two different techniques were used in this study. Adiabatic calorimetry was used to measure the heat capacity of $Nd_2Zr_2O_7$ powder in the temperature range of (3 to 400) K at Utrecht University. The apparatus (laboratory designation CAL V) and its calibration have been described previously [10]. Nine runs were made with this instrument and the results are presented in table 1. Measurements between $T = 0.45$ K and $T = 27$ K were made by a PPMS instrument (Quantum Design) at ITU using a hybrid adiabatic relaxation method. The apparatus was calibrated using NBS gold. Polycrystalline samples (pellet pieces) with the mass of 15 mg and 1.7 mg were used. The two-tau relaxation method was used to determine the heat capacity with PPMS software. The results of two runs are given in table 2.

3. Results and discussion

The results of the different runs by adiabatic calorimetry are in good agreement in the temperature range (10 to 400) K, as is shown in figure 1. At the low temperature

TABLE 1
Experimental heat capacity $C^0_{p,m}$ data for $Nd_2Zr_2O_7$ obtained with the adiabatic calorimeter at temperature T

T/K	$C^0_{p,m}$ / (J·K^{-1}·mol^{-1})	T/K	$C^0_{p,m}$ / (J·K^{-1}·mol^{-1})	T/K	$C^0_{p,m}$ / (J·K^{-1}·mol^{-1})	T/K	$C^0_{p,m}$ / (J·K^{-1}·mol^{-1})
Run 1							
297.03	231.7	321.08	237.8	347.92	244.6	374.81	249.9
298.15	231.1	324.06	238.6	350.90	245.2	377.80	250.4
300.21	231.5	327.04	239.4	353.89	245.8	380.79	251.0
303.20	232.6	330.02	240.2	356.87	246.5	383.79	251.7
306.18	233.2	333.01	241.0	359.86	247.0	386.79	252.3
309.16	234.1	335.99	241.7	362.85	247.5	389.79	252.7
312.14	235.2	338.97	242.4	365.84	248.2	392.79	253.1
315.12	236.2	341.95	243.2	368.82	248.9	395.79	253.7
318.10	237.0	344.94	243.9	371.82	249.3	398.79	254.4
Run 2							
119.67	131.0	167.49	172.3	220.71	203.2	271.18	223.3
121.32	132.5	170.44	174.3	223.67	204.6	274.16	224.4
123.61	134.8	173.39	176.3	226.64	206.0	277.13	225.4
126.53	137.8	176.34	178.3	229.60	207.4	280.10	226.5
129.44	140.6	179.28	180.2	232.57	208.7	283.08	227.6
132.34	143.4	182.24	182.1	235.53	210.0	286.05	228.6
135.25	146.1	185.19	184.0	238.50	211.2	289.02	229.6
138.17	148.8	188.14	185.6	241.46	212.5	292.00	230.7
141.09	151.3	191.09	187.4	244.43	213.7	294.98	231.7
144.01	153.9	194.05	189.2	247.40	214.9	297.96	232.6
146.94	156.4	197.01	190.9	250.36	216.1	300.93	233.3
149.87	158.9	199.97	192.5	253.33	216.9	303.92	234.2
152.80	161.2	202.93	194.2	256.31	217.7	306.90	235.2
155.73	163.5	205.89	195.7	259.29	219.0	309.88	236.0
158.66	166.3	211.81	198.8	262.26	220.0		
161.60	168.3	214.77	200.3	265.24	221.2		
164.55	170.2	217.74	201.7	268.21	222.3		
Run 3							
5.36	1.13	11.44	0.887	17.44	3.16	24.40	8.62
6.58	1.215	13.49	1.35	19.64	4.37	26.95	11.20
8.78	0.840	15.35	1.95	21.96	6.31	29.7	13.90
Run 4							
4.95	1.32	11.9	0.777	18.02	3.33	24.5	8.66
6.45	0.496	13.15	1.32	19.29	4.29	25.85	10.1
8.21	0.581	14.36	1.52	20.55	5.16	27.24	11.5
9.33	0.952	15.54	1.97	21.84	6.12	28.69	12.7
10.54	0.691	16.77	2.73	23.17	7.23	30.17	14.3
Run 5							
3.10	0.197	5.98	0.586	8.34	0.558	10.9	0.59
3.68	0.686	6.3	0.554	9.13	0.57	11.83	0.8
4.03	0.645	7.37	0.499	9.97	0.592	12.77	0.89
Run 6							
3.65	0.937	7.71	0.498	10.35	0.614	13.21	1.15
6.5	0.525	8.67	0.562	11.28	0.661	14.1	3.09
6.81	0.462	9.47	0.558	12.23	0.826		

TABLE 1 (*continued*)

T/K	$C^0_{p,m}$	T/K	$C^0_{p,m}$	T/K	$C^0_{p,m}$	T/K	$C^0_{p,m}$
	$(J \cdot K^{-1} \cdot mol^{-1})$		$(J \cdot K^{-1} \cdot mol^{-1})$		$(J \cdot K^{-1} \cdot mol^{-1})$		$(J \cdot K^{-1} \cdot mol^{-1})$
Run 7							
16.08	1.92	35.16	20.9	53.92	46.3	74.16	75.2
19.38	3.96	36.78	22.8	55.71	49.1	76.04	77.7
21.42	5.69	38.42	24.6	57.51	51.7	77.94	80.3
22.98	7.07	40.09	27.0	59.33	54.3	79.83	82.9
24.42	8.35	41.76	29.3	61.15	56.9	81.74	85.5
25.90	9.98	43.45	31.6	62.98	59.5	83.64	88.0
27.42	11.3	45.16	34.0	64.83	62.1	85.55	90.5
28.93	13.1	46.88	36.4	66.68	64.7	87.47	92.9
30.47	14.6	48.62	38.8	68.54	67.2	89.39	95.5
32.02	16.7	50.37	41.3	70.40	69.9		
33.58	18.8	52.14	43.8	72.28	72.6		
Run 8							
70.18	69.9	117.92	128.9	166.86	171.8	216.23	201.1
72.15	72.3	120.35	131.4	169.33	173.5	218.70	202.3
75.20	76.5	122.78	134.0	171.79	175.1	221.18	203.5
77.48	79.7	125.21	136.4	174.25	176.7	223.66	204.6
79.78	82.8	127.65	138.9	176.71	178.5	226.14	205.8
82.11	86.0	130.09	141.2	179.18	180.1	228.61	206.9
84.45	88.9	132.53	143.5	181.64	181.7	231.09	208.0
86.80	92.1	134.97	145.7	184.11	183.3	233.57	209.0
89.15	95.1	137.42	148.0	186.58	184.8	236.05	210.2
91.52	98.1	139.86	150.2	189.05	186.3	238.52	211.3
93.89	101.1	142.32	152.4	191.52	187.6	241.00	212.3
96.27	104.0	144.77	154.5	193.99	189.1	243.48	213.3
98.66	106.9	147.22	156.6	196.46	190.6	245.96	214.4
101.05	109.3	149.68	158.7	198.93	192.0	248.44	215.3
103.44	112.9	152.13	160.7	201.40	193.3	250.92	216.3
105.85	115.6	154.58	162.6	203.87	194.7	253.40	216.9
108.25	118.4	157.03	164.8	206.34	196.1	255.88	217.4
110.66	121.1	159.49	166.8	208.81	197.4	258.37	218.6
113.08	123.7	161.94	168.5	211.28	198.7	260.85	219.6
115.50	126.3	164.40	170.0	213.75	199.9		
Run 9							
262.50	220.0	298.46	232.7	335.64	242.3	372.91	250.0
263.89	220.6	300.95	232.6	338.12	243.0	375.40	250.6
266.37	221.6	303.46	231.9	340.60	243.3	377.89	251.0
268.83	222.2	305.94	234.6	343.08	243.9	380.38	251.3
271.30	223.2	308.41	235.2	345.57	244.6	382.87	251.9
273.77	224.1	310.88	235.9	348.05	245.2	385.37	252.3
276.23	225.1	313.35	236.5	350.53	245.6	387.86	252.8
278.70	225.8	315.83	237.3	353.01	246.2	390.36	253.5
281.17	226.9	318.30	238.0	355.50	246.6	392.86	253.8
283.64	227.8	320.77	238.5	357.98	247.2	395.36	254.3
286.11	228.9	323.25	239.1	360.47	247.6	397.86	254.7
288.57	229.5	325.73	239.8	362.95	248.1	400.37	255.1
291.05	230.3	328.20	240.7	365.44	248.7		
293.52	231.0	330.68	241.3	367.93	249.3		
295.99	232.0	333.16	241.6	370.42	249.6		

TABLE 2
Experimental heat capacity $C^0_{p,m}$ data for $Nd_2Zr_2O_7$ obtained with the hybrid adiabatic relaxation method at temperature T

T/K	$C^0_{p,m}$ / (J·K^{-1}·mol^{-1})	T/K	$C^0_{p,m}$ / (J·K^{-1}·mol^{-1})	T/K	$C^0_{p,m}$ / (J·K^{-1}·mol^{-1})	T/K	$C^0_{p,m}$ / (J·K^{-1}·mol^{-1})
Run 1							
1.884	1.234	3.664	0.486	5.772	0.256	9.644	0.316
1.931	1.198	3.712	0.470	5.875	0.250	9.745	0.325
1.977	1.164	3.757	0.461	5.976	0.246	9.847	0.334
2.025	1.132	3.804	0.451	6.078	0.242	9.949	0.344
2.073	1.099	3.848	0.447	6.182	0.239	10.051	0.354
2.119	1.069	3.897	0.437	6.282	0.236	10.153	0.365
2.166	1.037	3.944	0.427	6.385	0.233	10.165	0.367
2.214	1.008	3.988	0.419	6.488	0.230	10.668	0.428
2.260	0.982	4.038	0.412	6.591	0.228	11.184	0.504
2.308	0.958	4.082	0.407	6.692	0.226	11.700	0.596
2.355	0.934	4.129	0.397	6.794	0.224	12.220	0.706
2.402	0.909	4.175	0.393	6.895	0.223	12.741	0.832
2.449	0.887	4.221	0.386	6.998	0.222	13.261	0.978
2.495	0.863	4.270	0.377	7.094	0.222	13.792	1.147
2.542	0.842	4.314	0.373	7.194	0.221	14.299	1.325
2.590	0.818	4.361	0.369	7.298	0.221	14.816	1.529
2.635	0.797	4.407	0.361	7.398	0.222	15.341	1.754
2.683	0.778	4.452	0.360	7.501	0.222	15.882	2.000
2.729	0.756	4.499	0.353	7.603	0.223	16.414	2.271
2.775	0.738	4.546	0.348	7.707	0.224	16.926	2.540
2.821	0.721	4.593	0.341	7.808	0.226	17.444	2.829
2.868	0.704	4.637	0.338	7.911	0.228	17.966	3.135
2.914	0.682	4.685	0.335	8.013	0.230	18.493	3.465
2.960	0.665	4.731	0.331	8.114	0.232	19.019	3.803
3.015	0.653	4.776	0.326	8.217	0.235	19.537	4.196
3.060	0.634	4.822	0.320	8.318	0.237	20.059	4.578
3.107	0.619	4.872	0.315	8.421	0.241	20.591	4.989
3.154	0.602	4.918	0.311	8.527	0.245	21.117	5.397
3.201	0.591	4.963	0.307	8.627	0.249	21.641	5.823
3.248	0.572	5.010	0.302	8.730	0.254	22.155	6.259
3.294	0.568	5.057	0.298	8.831	0.259	22.677	6.726
3.341	0.553	5.109	0.295	8.933	0.265	23.236	7.242
3.386	0.549	5.161	0.290	9.034	0.271	23.735	7.699
3.433	0.534	5.262	0.284	9.137	0.277	24.234	8.194
3.478	0.514	5.365	0.277	9.238	0.284	24.770	8.705
3.525	0.513	5.467	0.270	9.339	0.291	25.278	9.229
3.570	0.504	5.568	0.265	9.440	0.299	25.823	9.800
3.617	0.492	5.671	0.260	9.542	0.307	26.337	10.355
Run 2							
0.465	4.277	0.611	3.419	0.914	2.539	1.420	1.686
0.478	4.143	0.626	3.384	0.964	2.462	1.471	1.625
0.493	3.941	0.642	3.327	1.015	2.347	1.525	1.575
0.508	3.982	0.656	3.282	1.066	2.238	1.571	1.529
0.523	3.869	0.663	3.229	1.117	2.152	1.621	1.471
0.537	3.666	0.671	3.206	1.167	2.081	1.670	1.424
0.552	3.717	0.713	3.054	1.217	2.008	1.721	1.381

TABLE 2 (*continued*)

T/K	$C^0_{p,m}$	T/K	$C^0_{p,m}$	T/K	$C^0_{p,m}$	T/K	$C^0_{p,m}$
	$(J\cdot K^{-1}\cdot mol^{-1})$		$(J\cdot K^{-1}\cdot mol^{-1})$		$(J\cdot K^{-1}\cdot mol^{-1})$		$(J\cdot K^{-1}\cdot mol^{-1})$
0.567	3.550	0.763	2.927	1.268	1.930	1.768	1.334
0.583	3.483	0.814	2.768	1.318	1.859	1.832	1.276
0.596	3.459	0.864	2.653	1.368	1.788		

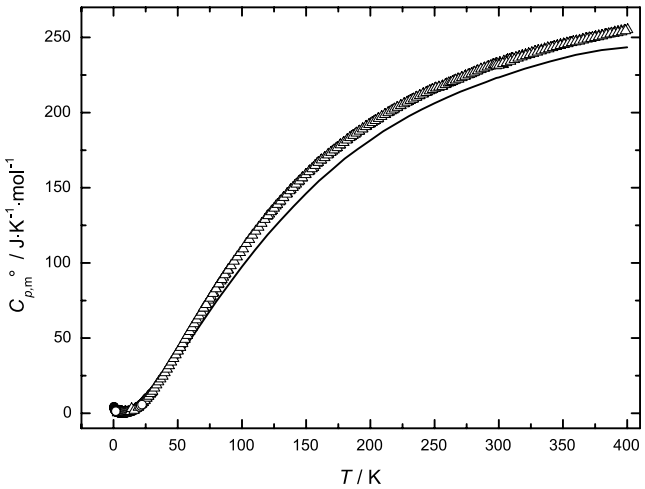

FIGURE 1. Heat capacity $C^0_{p,m}$ for $Nd_2Zr_2O_7$. Δ, Adiabatic calorimeter; ○, PPMS; —, reference [5] for $La_2Zr_2O_7$.

limit the data agree well with the results by PPMS whereas above $T = 300\,K$ they join smoothly with the high-temperature heat capacity ($T = 400\,K$ to $T = 1500\,K$) for this compounds measured by DSC [9].

The data obtained by PPMS show that the heat capacity does not continuously decrease with decreasing temperature but that it starts to rise at temperature below $T = 7.2\,K$ indicating the presence of a thermal anomaly shown in figure 2. Above $T = 7.2\,K$ the data join the adiabatic curve. Below $T = 7\,K$ the adiabatic data are scattered, which is due to the fact that the apparatus was operated at its lower temperature limit.

The Debye temperature was estimated to be $\theta_D = 489\,K$. The heat capacity data below the temperature of 25 K could be fitted to the equation $C^0_p = \alpha T^3$, except in the temperature range of the thermal anomaly, yielding $\alpha = 5.564\cdot 10^{-4}\,J\cdot K^{-4}\cdot mol^{-1}$. The plot of C^0_p/T versus T^2 below the temperature of 25 K is shown in figure 3. At $T = 7.2\,K$, the heat capacity $C^0_p(Nd_2Zr_2O_7, 7.2\,K) = 0.208\,J\cdot K^{-1}\cdot mol^{-1}$.

Figure 1 compares our results for $Nd_2Zr_2O_7$ to the heat capacity of lanthanum zirconate $La_2Zr_2O_7$ obtained by Bolech *et al.* [5,7] in the temperature range (20 to 400) K using the same adiabatic calorimeter. The $Nd_2Zr_2O_7$ curve is systematically higher than that of $La_2Zr_2O_7$. This difference corresponds to an excess component

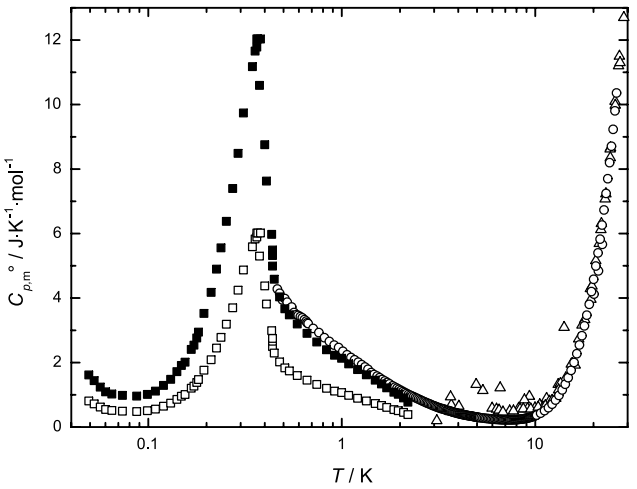

FIGURE 2. Heat capacity $C^0_{p,m}$ of $Nd_2Zr_2O_7$ between $T = 0\,K$ and $T = 25\,K$. △, by Adiabatic calorimeter; ○, PPMS; □, reference [14]; ■, reference [14] corrected for the number of Nd^{3+} ions in the structure as described in the text.

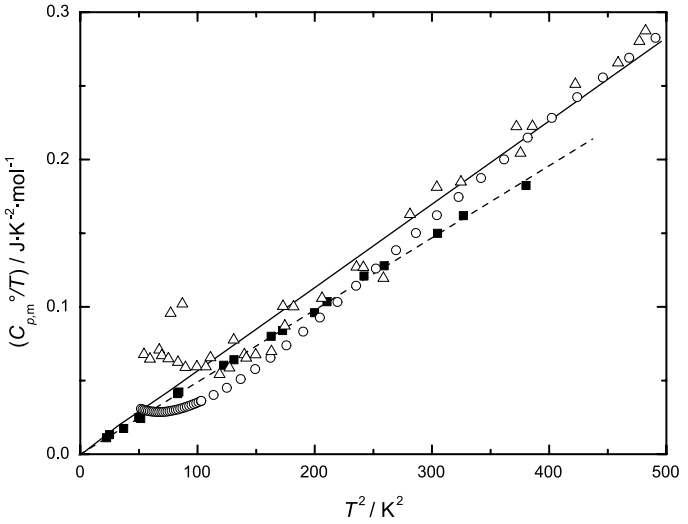

FIGURE 3. Low temperature heat capacity of $C^0_{p,m}$ $Nd_2Zr_2O_7$. Δ, Adiabatic calorimeter; ○, PPMS; ——, αT^3 fit; ■, reference [5] for $La_2Zr_2O_7$; - - -, αT^3 fit to the results from reference [5].

to the heat capacity C_{exs}, a so-called Schottky anomaly, that arises from the lowering of the magnetic ordering (splitting of the ground term) by the crystalline electric field (Stark effect) [11]. The Nd^{3+} ion has a $4f^3$ electronic configuration and the ground state of the free ion is $^4I_{9/2}$ ($g_0 = 10$) which in the ionic crystal lattice splits into five

Kramers doublets ($g = 2$). Lanthanum zirconate has no excess component in this temperature range due to very stable $4f^0$ electronic configuration of the La^{3+} ion, and its heat capacity consists only of the lattice component. Thus the total heat capacity C_p^0 is given by

$$C_p^0 = C_{lat} + C_{exs}, \tag{1}$$

where C_{lat} is the lattice contribution to the heat capacity. The excess component of neodymium zirconate can be approximately deduced from the difference with the heat capacity of lanthanum zirconate. The data obtained from $T = 20\,K$ to $T = 400\,K$ reveal the Schottky anomaly to the heat capacity.

The excess component can also be calculated from the crystal field energies according the equation [12]

$$C_{exs} = Q^{-2}R^{-1}T^{-2}\left[Q\sum_{i=1}^{n} g_i E_i^2 \exp(-E_i/RT) - \left\{\sum_{i=1}^{n} g_i E_i \exp(-E_i/RT)\right\}^2\right], \tag{2}$$

where Q is the partitioning function described in equation (3) by the Maxwell–Boltzmann distribution law, T the temperature, R the universal gas constant, and E_i the energy of the level i, and g_i its degeneracy.

$$Q = \sum_{i=0}^{n} g_i \exp(-E_i/RT). \tag{3}$$

As a first approximation the excess component was calculated from the energy levels of Nd^{3+} in Nd_2O_3 or $NdAlO_3$ [13], as the crystal field splitting in $Nd_2Zr_2O_7$ is not known. However, poor agreement with the experimental values for $Nd_2Zr_2O_7$ was observed, indicating that the crystal field energy of the Nd^{3+} ion in the pyrochlore structure are significantly different from those in these two compounds.

Figure 2 shows the heat capacity measured by both techniques in the temperature range (0.45 to 20) K using a logarithmic temperature scale. Only the high-temperature tail of an anomaly is present in our results, the remainder of the peak occurs below the lower temperature limit of the PPMS apparatus. This anomaly should be considered as the onset of a cooperative transition to remove the ground state degeneracy of the doublet.

Also shown in the figure are the heat capacity data for the same compound reported by Blöte *et al.* [14] in the temperature range (0.05 to 3) K. These authors observed the maximum in the anomaly at $T = 0.37\,K$, whereas they cite the work of van Geuns who found a Curie temperature around $T = 0.6\,K$ from magnetic susceptibility measurements. Our results are systematically higher than those of Blöte *et al.* [14], but the interpretation of their results is not fully clear, as we will discuss in the next section.

Similar to the heat capacity, the entropy S^0 is described as the sum of a lattice component S_{lat} and an excess component S_{exs} [11]

$$S^0 = S_{lat} + S_{exs}. \tag{4}$$

TABLE 3
Thermodynamic functions of $Nd_2Zr_2O_7$ from $T = 10\,K$ to $T = 400\,K$ ($\Phi^0_m = [\Delta G^0_m(T) - \Delta H^0_m(0)]/T$)

T/K	$C^0_{p,m}$	$S^0_m(T)$	$\Delta^T_{298.15}H_m(T)$	Φ^0_m
	$(J \cdot K^{-1} \cdot mol^{-1})$	$(J \cdot K^{-1} \cdot mol^{-1})$	$(J \cdot mol^{-1})$	$(J \cdot K^{-1} \cdot mol^{-1})$
10	0.354	12.76	8.76	11.88
15	1.61	13.09	13.04	12.22
20	4.70	13.92	27.9	12.52
25	9.41	15.43	62.0	12.95
30	14.18	17.53	120.1	13.53
35	20.69	20.20	206.9	14.29
40	26.88	23.34	325.1	15.21
45	33.74	26.91	476.7	16.32
50	40.80	30.83	663.0	17.57
55	47.98	35.05	884.6	18.97
60	55.25	39.54	1143	20.49
65	62.35	44.24	1437	22.13
70	69.29	49.12	1766	23.89
75	76.31	54.14	2130	25.74
80	83.09	59.28	2529	27.67
85	89.68	64.52	2961	29.68
90	96.18	69.83	3426	31.76
95	102.5	75.20	3922	33.92
100	108.2	80.60	4449	36.11
110	120.4	91.48	5592	40.65
120	131.2	102.4	6850	45.34
130	141.1	113.3	8212	50.15
140	150.3	124.1	9669	55.05
150	159.0	134.8	11215	60.01
160	167.2	145.3	12846	65.01
170	174.0	155.6	14552	70.03
180	180.7	165.8	16326	75.07
190	186.8	175.7	18163	80.11
200	192.5	185.4	20060	85.13
210	198.0	195.0	22012	90.13
220	202.9	204.3	24017	95.11
230	207.5	213.4	26069	100.1
240	211.9	222.3	28166	105.0
250	216.0	231.1	30305	109.8
260	219.3	239.6	32482	114.7
270	222.8	248.0	34692	119.4
280	226.4	256.1	36938	124.2
290	229.9	264.1	39220	128.9
298.15	232.7	270.5	41105	132.6
300	233.1	272.0	41535	133.5
310	236.0	279.6	43881	138.1
320	238.4	287.2	46253	142.6
330	241.1	294.6	48650	147.1
340	243.2	301.8	51072	151.6
350	245.5	308.9	53515	156.0
360	247.5	315.8	55980	160.3
370	249.5	322.6	58465	164.6
380	251.3	329.3	60969	168.8
390	253.4	335.84	63493	173.0

For the same reasons as mentioned earlier, the lattice entropy of neodymium zirconate can be represented by the entropy of lanthanum zirconate. The heat capacity of $La_2Zr_2O_7$ was fitted to $C_p^0(La_2Zr_2O_7) = 4.895 \cdot 10^{-4}(T/K)^3$ in the temperature range (0 to 25) K. The value $S^0(La_2Zr_2O_7, 7.2\,K) = S_{lat}(Nd_2Zr_2O_7, 7.2\ K) = 0.0609\,J \cdot K^{-1} \cdot mol^{-1}$ was obtained by integration of $C_p^0(La_2Zr_2O_7)/T$ from $T = 0\,K$ to $T = 7.2\,K$.

The excess component of the entropy can be calculated from the crystal field energies according the equation

$$S_{exs} = R\ln(g_0) + R\ln\left\{\sum_{i=1}^{n} g_i \exp(-E_i/RT)\right\}. \quad (5)$$

The first term represents the contribution of the ground state, the second term that of the crystal field energies, which is only relevant at temperatures above $T = 10\,K$ for $Nd_2Zr_2O_7$ (as the first excited state is very probably >100 cm^{-1}). As discussed above, the ground state of the Nd^{3+} ion in $Nd_2Zr_2O_7$ is a doublet ($g = 2$) and thus $S_{exs}(Nd_2Zr_2O_7, 7.2\,K) = 2R\ln(2) = 11.526\,J \cdot K^{-1} \cdot mol^{-1}$.

Blöte *et al.* [14] reported $\Delta S/R = 0.698 = 1.007\ln(2)$ for the entropy of the low temperature anomaly in $Nd_2Zr_2O_7$, and argued that this is an indication for a doublet ground state. However, it is a factor 2 lower than the theoretical value, which probably means that they normalised their results to one mole of Nd^{3+} ions. The heat capacity of $Nd_2Zr_2O_7$ obtained by doubling the experimental values of Blöte *et al.* is plotted in figure 2, which shows that a very good agreement with the experimental values measured by PPMS is now obtained.

The total molar entropy of $Nd_2Zr_2O_7$ at $T = 7.2\,K$ is the sum of these two terms (lattice and excess components) yielding $S^0(Nd_2Zr_2O_7, 7.2\,K) = 11.587\,J \cdot K^{-1} \cdot mol^{-1}$. Using this value the thermodynamic functions of $Nd_2Zr_2O_7$ in the temperature range (10 to 400) K were derived, as summarised in table 3. The value obtained for the heat capacity and the entropy at the standard temperature of 298.15 K are $C_p^0(Nd_2Zr_2O_7, 298.15\,K) = (232.7 \pm 0.3)\,J \cdot K^{-1} \cdot mol^{-1}$ and $S^0(Nd_2Zr_2O_7, 298.15\,K) = (264.1 \pm 0.6)\,J \cdot K^{-1} \cdot mol^{-1}$.

4. Conclusion

The thermodynamic functions of $Nd_2Zr_2O_7$ pyrochlore were obtained from the low temperature heat capacity measurements. The excess component of the heat capacity was determined by assuming the heat capacity of $La_2Zr_2O_7$ to represent the lattice component of $Nd_2Zr_2O_7$. The resulting values were compared with calculations using the crystal field energies of the Nd^{3+} ion in Nd_2O_3 and $NdAlO_3$. The significant difference between the experimental and calculated data is probably due to two facts: the lattice component is not constant over the lanthanide series, and the energy levels of the Nd^{3+} are different in the pyrochlore structure. In order to better resolve the lattice and the excess component of the heat capacity for the lanthanide zirconate pyrochlore series, measurements of the heat capacity of some other

lanthanide zirconates (Ln = Eu and Gd) by the same techniques and the determination of the energy levels of lanthanide ions in the pyrochlore structure by optical spectroscopy are currently in progress and will be discussed in a following paper.

Acknowledgements

We would like to thank J.G. Boshoven, H. Hein, A. Fernandez, and R. Voet for their assistance for the samples preparation, S.L. and P.J. acknowledge the European Commission for support given in the frame of the program "training and mobility of researchers".

References

[1] M.A. Subramanian, G. Aramudan, G.V. Subba Rao, Prog. Solid State Chem. 15 (1983) 55–143.
[2] B.F. Woodfield, J. Boerio-Goates, J.L. Shapiro, R.L. Putnam, A. Navrotsky, J. Chem. Thermodyn. 31 (1999) 245–253.
[3] R.L. Putnam, A. Navrotsky, B.F. Woodfield, J. Boerio-Goates, J.L. Shapiro, J. Chem. Thermodyn. 31 (1999) 229–243.
[4] V.R. Korneev, V.B. Glushkova, E.K. Keler, Izv. Akad. Nauk SSSR, Neorg. Mater. 7 (1971) 886–887.
[5] M. Bolech, Ph.D. Thesis, University of Amsterdam, Amsterdam, Netherlands, 1998.
[6] M. Bolech, E.H.P. Cordfunke, F.J.J.G. Janssen, A. Navrotsky, J. Am. Ceram. Soc. 78 (1995) 2257–2258.
[7] M. Bolech, E.H.P. Cordfunke, A.C.G. Van Genderen, R.R. Van Der Laan, F.J.J.G. Janssen, J.C. Van Miltenburg, J. Phys. Chem. Solids 58 (1997) 433–439.
[8] K.B. Helean, B.D. Begg, A. Navrotsky, B. Ebbinghaus, W.J. Weber, R.C. Ewing, Mat. Res. Soc. Symp. Proc. 663 (2001) 691–697.
[9] S. Lutique, R.J.M. Konings, V.V. Rondinella, J. Somers, T. Wiss, J. Alloy Compd. 352 (2003) 1–5.
[10] J.C. Van Miltenburg, G.J.K. van den Berg, M.J. van Bommel, J. Chem. Thermodyn. 19 (1987) 1129–1138.
[11] R.J.M. Konings, J. Nucl. Mater. 295 (2001) 57–63.
[12] B.H. Justice, E.F.J. Westrum, J. Phys. Chem. 67 (1963) 339–345.
[13] C.A. Morrison, R.P. Leavitt, in: K.A. Gschneidner, L. Eyring Jr. (Eds.), Handbook of the Physics and Chemistry of Rare Earth, vol. 5, 1982 (Chapter 46).
[14] H.W.J. Blöte, R.F. Wielinga, W.J. Huiskamp, Physica 43 (1969) 549–568.

AG02/025